LETTER

doi:10.1038/nature09958

Stem–cell–triggered immunity through CLV3p–FLS2 signalling

Horim Lee[1], Ok-Kyong Chah[1] & Jen Sheen[1]

Stem cells in the shoot apical meristem (SAM) of plants are the self-renewable reservoir for leaf, stem and flower organogenesis[1,2]. In nature, disease-free plants can be regenerated from SAM despite infections elsewhere, which underlies a horticultural practice for decades[3]. However, the molecular basis of the SAM immunity remains unclear. Here we show that the CLAVATA3 peptide (CLV3p), expressed and secreted from stem cells and functioning as a key regulator of stem-cell homeostasis in the SAM of *Arabidopsis*[1,2,4], can trigger immune signalling and pathogen resistance via the flagellin receptor kinase FLS2 (refs 5, 6). CLV3p–FLS2 signalling acts independently from the stem-cell signalling pathway mediated through CLV1 and CLV2 receptors[1,2,4], and is uncoupled from FLS2-mediated growth suppression[5,6]. Endogenous CLV3p perception in the SAM by a pattern recognition receptor for bacterial flagellin, FLS2, breaks the previously defined self and non-self discrimination in innate immunity[6,7]. The dual perception of CLV3p illustrates co-evolution of plant peptide and receptor kinase signalling for both development and immunity. The enhanced immunity in SAM or germ lines may represent a common strategy towards immortal fate in plants and animals[1,2,8].

In both plants and animals, innate immunity is triggered through pattern recognition receptors (PRRs) in response to microbe-associated molecular patterns (MAMPs)[6,7] to provide the first line of inducible defence. Plant receptor kinases represent the main functions of known plasma membrane PRRs for MAMP recognition to distinguish non-self from self[6]. FLS2 is the first characterized plant leucine-rich-repeat (LRR) receptor kinase that perceives bacterial flagellin and launches convergent downstream signalling and defence pathways for potentially broad-spectrum pathogen resistance[5,6,9–11]. The perception of bacterial flagellin is conserved in seed plants, and functional FLS2 orthologues are found from *A. thaliana* to rice[5,6]. As *FLS2* is expressed throughout the whole plant including the SAM (Supplementary Fig. 2)[5,12], flagellin–FLS2 signalling could provide immune protection in different parts of the plant body after infections.

While developing a plant expression system to screen for peptide-mediated receptor-like kinase (RLK) signalling, we observed that the endogenously modified 12-amino-acid CLV3p (Supplementary Table 1)[13] triggered similar responses as flg22 (the conserved 22-amino-acid peptide of bacterial flagellin) in mesophyll protoplasts[5,6,9,14–16]. This finding was unexpected because CLV3p is normally expressed, secreted and processed by the stem cells to control SAM maintenance via CLV1 and CLV2 receptors[1,2,4,13,17]. Flg22 and CLV3p, but not ΔCLV3p lacking the last His residue, activated similar mitogen-activated protein kinase (MAPK) activities detected by the in-gel kinase assay (Fig. 1a and Supplementary Fig. 3)[6,9,14–16]. Highly purified CLV3p synthesized by different sources displayed the same activities, ruling out the contamination possibility. We sought to identify the CLV3p receptor in leaf cells by examining MAPK activation in various receptor mutants. Neither the dominant *clv1-1* mutant (Fig. 1a) nor the *clv2-1* mutant (Supplementary Fig. 4)[1,2,4,17–19] affected CLV3p-triggered MAPK activation. Surprisingly, two independent *fls2* mutant alleles of Landberg *erecta* (L*er*) and Columbia (Col-0)[5,6], but not the *efr-1* (the bacterial elongation factor EF-Tu receptor EFR) mutant[20], failed to support the activation of MAPKs by both flg22 and CLV3p (Fig. 1a and Supplementary Fig. 3). Complementation with the wild-type *FLS2* gene (Fig. 1b), but not *CLV1* (data not shown) in the *fls2* mutant, confirmed that FLS2 could recognize both flg22 and CLV3p to mediate MAPK signalling. Importantly, CLV3p and flg22 activated similar early marker genes, including *FRK1*, *WRKY29* and *WRKY30* (Fig. 1c)[9,10,14].

FLS2 signalling requires the recruitment of the RLK BAK1 and the interaction between FLS2 and BAK1 represents the earliest event (within a minute) triggered by flg22 binding to FLS2 (refs 6, 14–16). Like flg22, CLV3p also induced the immediate interaction between FLS2 and BAK1 detected by reciprocal co-immunoprecipitation (Supplementary Fig. 5a, b)[14–16]. Consistently, CLV3p signalling monitored by MAPK activation was greatly diminished in the *bak1-4* mutant (Supplementary Fig. 6)[14–16]. Notably, CLV3p pre-treatment could confer enhanced resistance to the pathogenic bacteria *Pseudomonas syringae* pv. *tomato* DC3000 in an FLS2-dependent manner (Fig. 1d)[10,14]. These comprehensive analyses strongly support our new finding that the conserved flagellin receptor FLS2 can recognize the stem-cell peptide CLV3p and trigger convergent innate immune signalling[6,9,14].

Peptide titration experiments using the FLS2 and BAK1 co-immunoprecipitation assay showed that 1 nM flg22 was as potent as 1 μM CLV3p (Fig. 2a and Supplementary Fig. 5c) required for SAM suppression[13,21]. Intriguingly, flg22 and CLV3p peptides supported similar primary gene activation but distinct long-term growth effects

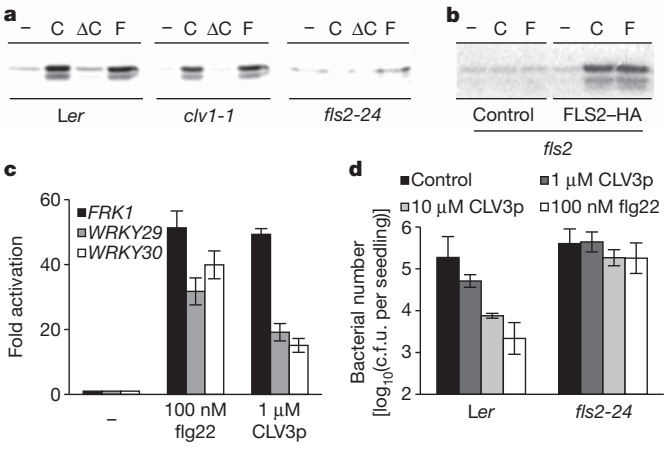

Figure 1 | CLV3p and flg22 activate similar downstream responses through FLS2. **a**, MAPK activity analysis. L*er*, *clv1-1* and *fls2-24* protoplasts were treated with 1 μM CLV3p (C), 1 μM ΔCLV3p (ΔC) or 100 nM flg22 (F) for 10 min. **b**, FLS2–HA complements *fls2*. **c**, CLV3p triggers flg22 marker gene activation. Quantification by qRT–PCR; peptide treatment for 1 h. Error bars indicate s.d. ($n = 3$). **d**, CLV3p enhances resistance to *P. syringae* pv. *tomato* DC3000. Error bars indicate s.d. ($n = 3$). c.f.u., colony-forming units.

[1]Department of Molecular Biology and Center for Computational and Integrative Biology, Massachusetts General Hospital, and Department of Genetics, Harvard Medical School, Boston, Massachusetts 02114, USA.

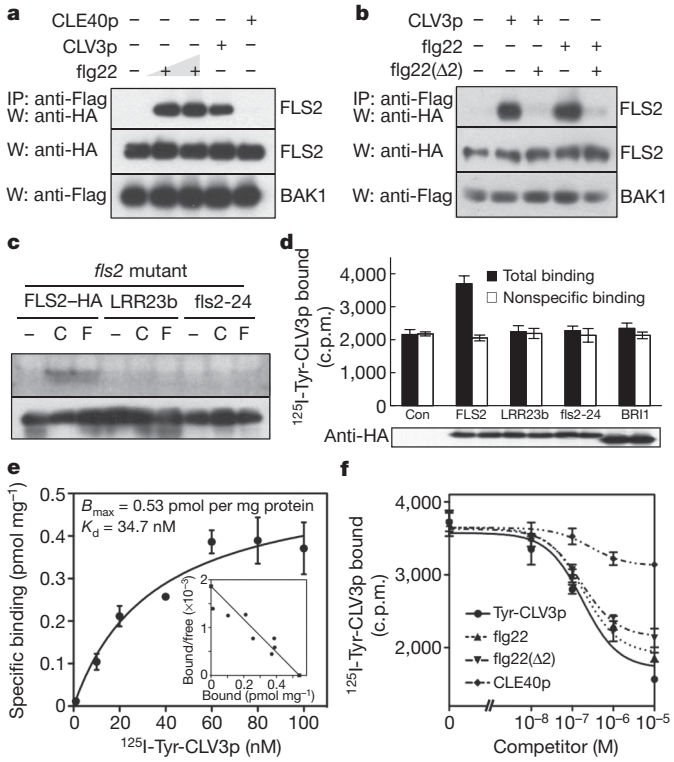

Figure 2 | CLV3p and flg22 share similar perception through FLS2. **a**, CLE40p fails to induce FLS2–BAK1 interaction. Treatments: flg22 (1, 10 nM), 1 μM CLV3p or 1 μM CLE40p for 10 min. **b**, Flg22(Δ2) blocks CLV3p and flg22 signalling. Flg22(Δ2) (50 μM). **c**, LRR mutations of FLS2 eliminate flg22 and CLV3p perceptions in *fls2*. Top, in-gel kinase assay; bottom, protein expression. **d**, ^{125}I-Tyr-CLV3p specifically binds to FLS2. Nonspecific binding (20 μM unlabelled Tyr-CLV3p). Error bars indicate s.d. ($n = 3$). c.p.m., counts per min. **e**, Saturation binding curve and Scatchard plot. Error bars indicate s.d. ($n = 3$). **f**, Binding competition analysis with peptides. Error bars indicate s.d. ($n = 3$). Nonspecific binding (10 μM unlabelled Tyr-CLV3p).

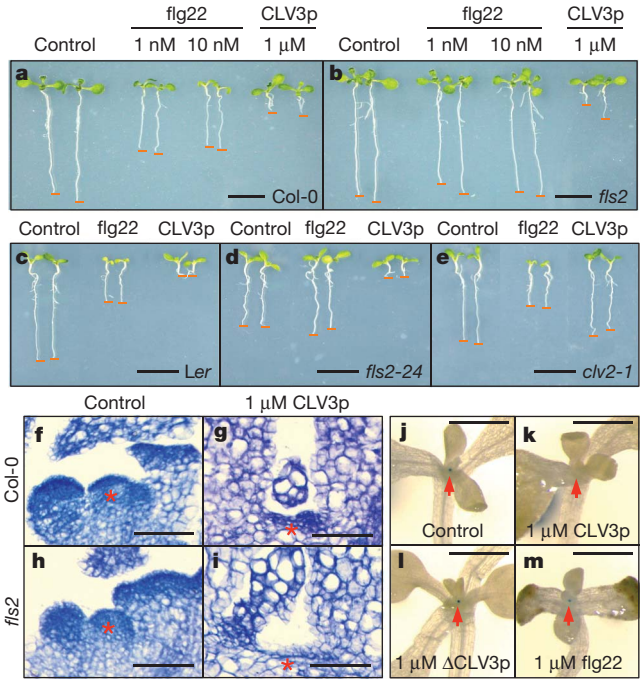

Figure 3 | CLV3p-mediated SAM arrest and immune signalling are uncoupled from flg22-triggered growth suppression. **a**–**e**, Growth inhibition analysis. Treatment with flg22 (1, 10 nM) or CLV3p (1 μM) in Col-0 (**a**), *fls2* (**b**), *Ler* (**c**), *fls2-24* (**d**) and *clv2-1* (**e**) seedlings. Scale bars, 1 cm. **f**–**i**, CLV3p suppresses the SAM in Col-0 and *fls2* plants. Red asterisks indicate SAM region. Scale bars, 50 μm (**f**–**i**). **j**–**m**, CLV3p represses *pWUS::GUS* expression. Treatment was without (**j**) or with 1 μM CLV3p (**k**), 1 μM ΔCLV3p (**l**) or 1 μM flg22 (**m**). Red arrows indicate SAM region. Scale bars, 1 mm.

in seedling assays (Figs 3 and 4 and Supplementary Fig. 7). Flg22 is a MAMP from non-self invaders and is detected by a very sensitive perception system[22] to induce innate immunity in a timely manner after infection. CLV3p, on the other hand, is an endogenous plant signal naturally secreted in the stem-cell zone to activate constitutive innate immunity via FLS2 in the SAM, which might provide a type of 'vaccination' before any infections to elicit sufficient immune protection without severe growth penalty caused by MAMPs (Fig. 3a–e)[5,6,15,20].

CLV3 belongs to the *CLV3/ERS*-related (*CLE*) gene family, which is conserved in diverse plant species[4,17–19]. The *Arabidopsis* genome has 32 *CLE* genes[4,17–19]. CLV3p and many other CLE peptides share similar root growth inhibition activity through the CLV2–CRN (CORYNE)/SOL2 (SUPPRESSOR OF OVEREXPRESSION OF LLP1-2) receptor complex, revealing a high degree of redundancy in peptide signalling[18,19]. To assess the specificity of CLV3p–FLS2 signalling, we examined the activity of synthetic peptide CLE40p, which belongs to the same CLE subgroup as CLV3p (refs 4, 17, 18, 21). CLE40p triggered the growth arrest of SAM, repression of *WUSCHEL* (*WUS*) detected by *pWUS::GUS* (ref. 23), and root growth inhibition (Supplementary Fig. 8a, b) as previously reported for CLV3p and CLE19p (refs 4, 17, 18, 21). *WUS* encodes a homeodomain transcription factor that has a central role in *Arabidopsis* SAM maintenance[1,2]. However, CLE40p did not promote FLS2–BAK1 interaction or flg22 early marker gene activation (Fig. 2a and Supplementary Fig. 8c). CLV3p–FLS2 signalling might be unique among CLE peptides.

To determine whether flg22- and CLV3p-triggered FLS2 signalling through the same or different extracellular sites, we carried out competition experiments using a well-established antagonist peptide lacking only the last two amino acids at the carboxy terminus of flg22 (flg22(Δ2))[24]. On the basis of the CLV3p- or flg22-triggered FLS2–BAK1 interaction assay by co-immunoprecipitation, we showed that flg22(Δ2) effectively competed with and blocked flg22 and CLV3p signalling (Fig. 2b). Moreover, two LRR mutants, one in the 10th LRR domain (*fls2-24*) and the other in the 23rd LRR domain (the *LRR23b* mutant) of FLS2, failed to activate flg22 and CLV3p signalling detected by MAPK activation despite normal FLS2 protein levels (Fig. 2c)[9,14–16,24–26]. These results indicate that flg22 and CLV3p probably share binding and activation sites in the extracellular LRR domain of FLS2.

On the basis of the established studies on the flg22–FLS2 and CLV3p–CLV1 interactions[27,28], we developed a cell-based assay to show that ^{125}I-Tyr-CLV3p interacted directly with FLS2 expressed in the null *fls2* mutant protoplasts. Importantly, only the wild-type FLS2 protein but not the fls2-24 and LRR23b mutant protein or the brassinosteroid receptor kinase (BRI1) showed specific binding to ^{125}I-Tyr-CLV3p (Fig. 2d). The saturation binding curve and Scatchard plot were generated using the specific binding assay. The estimated dissociation constant (K_d) for FLS2 and ^{125}I-Tyr-CLV3p interaction was 34.7 nM (Fig. 2e), which was close to the K_d for CLV1 and CLV3p interaction[28]. The specific binding could be competed by the unlabelled Tyr-CLV3p, CLV3p, flg22, flg22(Δ2), but not CLE40 (Fig. 2f and Supplementary Fig. 9). Tyr-CLV3p and CLV3p displayed identical effectiveness in competing with ^{125}I-Tyr-CLV3p for binding to FLS2 (Supplementary Fig. 9), immune marker gene activation and root inhibition (data not shown). ^{125}I-Tyr-CLV3p binding to FLS2 shared characteristics of CLV3p binding to CLV1 (ref. 28). Although the estimated K_d for ^{125}I-Tyr-flg22 binding to FLS2 is lower[27] and FLS2 responses to flg22 are more sensitive (Figs 1c, d and 2a, and Supplementary Fig. 5a, c), flg22 did not compete more effectively than Tyr-CLV3p and CLV3p for ^{125}I-Tyr-CLV3p binding to FLS2. Because the sequences of CLV3p and flg22 do not share any overt similarity and ΔCLV3p was ineffective in activating or blocking FLS2 signalling

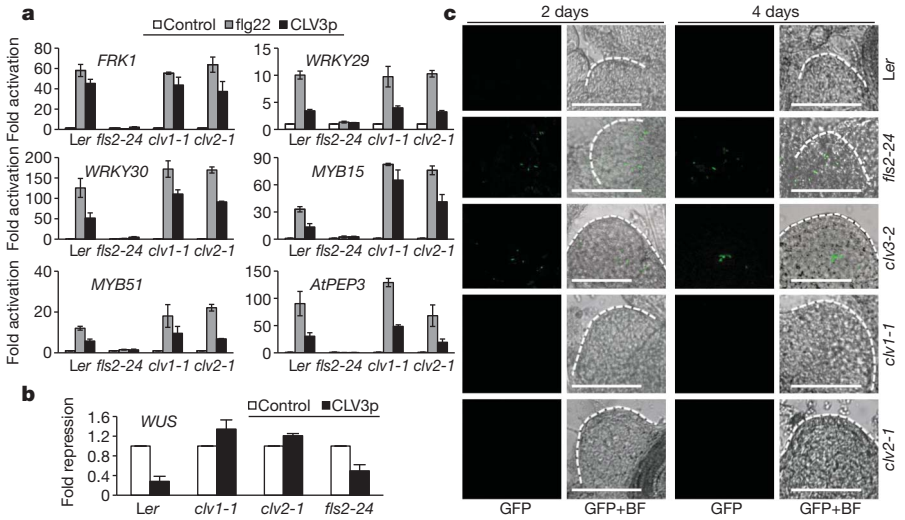

Figure 4 | CLV3p–FLS2 signalling enhances innate immunity for SAM protection. **a**, Flg22 marker gene activation by CLV3p through FLS2 in the SAM. **b**, *WUS* repression by CLV3p was mediated via CLV1 or CLV2 but not FLS2. The SAM tissues were analysed by qRT–PCR after treatment with 1 nM flg22 or 1 μM CLV3p for 1 h. Error bars indicate s.d. ($n = 3$). **c**, Infection and proliferation of pathogenic bacteria in the SAM lacking CLV3p–FLS2 signalling. *P. syringae* pv. *tomato* DC3000–GFP was co-cultivated with seedlings for 2 or 4 days. *P. syringae* pv. *tomato* DC3000–GFP was visualized using a confocal microscope. Scale bars, 50 μm. BF, bright field.

(Fig. 1a, data not shown), it was surprising to discover that they could still compete for some potentially shared binding sites on the LRR of FLS2 (Fig. 2b, c, f). The precise location of flg22 and CLV3p binding to FLS2 awaits future co-crystallographic analysis or mass spectrometry studies on cross-linked ligand–receptor complexes.

In previous studies, innate immune responses and growth inhibition are always tightly linked[5,6,15,20]. We investigated the effects of flg22 and CLV3p on seedling growth[5,6,15,20]. Surprisingly, CLV3p did not inhibit shoot growth but caused stronger root growth arrest in Col-0 and L*er* wild-type seedlings (Fig. 3a, c and Supplementary Figs 7a and 8b). Whereas seedling growth inhibition in both shoots and roots by flg22 was eliminated in two independent *fls2* mutants, the stronger root growth arrest by CLV3p was retained (Fig. 3b, d). Although CLV3p activated, via FLS2, a spectrum of innate immune responses similar to those via flg22–FLS2 signalling in mesophyll cells, seedlings and the SAM (Figs 1, 2 and 4 and Supplementary Figs 3, 5 and 8), CLV3p did not stimulate the typical flg22–FLS2-mediated growth suppression in whole seedlings (Fig. 3a–e). Similar to other synthetic CLE peptides, CLV3p-triggered root growth arrest was abolished in the *clv2-1* mutant (Fig. 3c–e and Supplementary Fig. 7)[18,19]. Thus, CLV3p–FLS2 signalling activated only immune responses but not the general growth inhibition. Significantly, CLV3p was very active in triggering the typical SAM arrest in null *fls2* seedlings (Fig. 3f–i)[1,2,4,13,17–19,23,28]. The SAM growth arrest was correlated with the repression of a sensitive *pWUS::GUS* reporter in the organizing centre by the exogenous CLV3p but not ΔCLV3p or flg22 (Fig. 3j–m)[23].

Because CLV3p is specifically expressed and secreted from stem cells of the SAM[1,2,4,13,17,23], it is critical to examine CLV3p–FLS2 signalling in the SAM to evaluate its physiological relevance. Using quantitative real-time reverse transcriptase PCR (qRT–PCR) analysis with isolated SAM tissues, CLV3p clearly triggered two parallel signalling pathways in the SAM (Fig. 4a, b and Supplementary Figs 10–13). The activation of important immune marker genes by CLV3p in wild type, *clv1-1*, *clv2-1* but not *fls2-24* validated the action of innate immune signalling via FLS2 in the *Arabidopsis* SAM. These flg22 and CLV3p inducible genes, including *FRK1* (a RLK), *WRKY29*, *WRKY30*, *MYB15*, *MYB51* (transcription factors) and *PEP3* (a peptide inhibiting *P. syringae* pv. *tomato* DC3000 growth via RLK signalling), have important roles in bacterial and fungal resistance[6,9,10,14]. Consistently, some of these marker genes showed reduced endogenous expression in the SAM of *clv3-2*, but were constitutively expressed at higher levels in the SAM but not other tissues of wild type (Supplementary Figs 10, 11a and 12). Their endogenous expression levels were low in both the SAM and other tissues in *clv3-2* and *fls2-24* (Supplementary Fig. 12). Complementation of *clv3-2* for immune marker gene expression in the SAM could be achieved with nanomolar range of exogenous CLV3p, reflecting the physiological relevance of the K_d for CLV3p and FLS2 interaction and CLV3p–FLS2 signalling in the SAM (Fig. 2e and Supplementary Fig. 10). The flg22 induction of these immune marker genes was observed in the SAM of *clv1-1*, *clv2-1* and *clv3-2* mutants, supporting the potency of MAMP signalling via FLS2 (Fig. 4a and Supplementary Fig. 11b). At 10–100 pM flg22, the immune marker gene induction levels were reduced in the SAM of *clv3-2* compared to those in the SAM of wild type and *clv1-1*, indicating the operation of both CLV3p–FLS2 and flg22–FLS2 signalling pathways in the SAM (Supplementary Fig. 13). The repression of *WUS* was triggered by CLV3p only in the SAM of wild type and *fls2-24*, but not *clv1-1* and *clv2-1* (Fig. 4b)[1,2,4,17,19,23].

Most notably, we have never detected the presence of a single live *P. syringae* pv. *tomato* DC3000–GFP bacterium in the SAM of wild-type seedlings in 11 infection experiments by visualizing bacteria proliferation using confocal microscopy for up to 4 days (Fig. 4c and Supplementary Fig. 14a). Because *P. syringae* pv. *tomato* DC3000–GFP could be easily visualized in the infected wild-type and *clv3-2* cotyledons (Supplementary Fig. 14b, d), the wild-type SAM appeared to exhibit differential immunity (Fig. 4c and Supplementary Fig. 14a). Notably, the SAM was no longer protected from *P. syringae* pv. *tomato* DC3000–GFP infection in *fls2-24* and *clv3-2* mutants (Fig. 4c and Supplementary Fig. 14c, e, f), supporting the important role of endogenous CLV3p in protection of the SAM through the FLS2-mediated innate immune signalling pathway (Fig. 4c and Supplementary Figs 1 and 14). To demonstrate further and quantify the proliferation and growth of *P. syringae* pv. *tomato* DC3000–GFP in the SAM of the *fls2-24* and *clv3-2* mutants observed after 2–4 days of infection, we counted the increasing bacteria numbers and carried out quantitative PCR analysis of the GFP DNA from the bacteria, both indicating the loss of the distinct SAM immunity (Fig. 4c and Supplementary Figs 14e and 15). There were higher numbers of *P. syringae* pv. *tomato* DC3000–GFP bacteria in the bigger *clv3-2* SAM with more cells of similar size but not bigger cells (Supplementary Fig. 14c, e). Importantly, *P. syringae* pv. *tomato* DC3000–GFP was found to be completely excluded from the similarly enlarged *clv1-1* and *clv2-1* SAM, in which CLV3p–FLS2 signalling remained active (Fig. 4c). On the basis of the qPCR analysis of GFP DNA derived only from *P. syringae* pv. *tomato* DC3000–GFP, nonspecific bacteria attachment background could be

estimated from the SAM tissue samples 1 h after bacteria–seedling co-cultivation. Consistent with confocal microscopic observations, active bacteria growth and proliferation were exclusively detected only in the SAM of the *clv3-2* and *fls2-24* mutants (Supplementary Fig. 15).

We have uncovered a surprising mechanism underlying the stem-cell-triggered immunity for pathogenic bacteria through CLV3p–FLS2 signalling (Supplementary Fig. 1). It will be interesting to examine the SAM protection from a variety of other pathogens. We propose that CLV3p is recognized by two distinct types of receptors involved in mostly non-overlapping functions in the SAM (Supplementary Fig. 1). The 'constitutive' immunity in the SAM resembles flg22 pre-treatment as a type of vaccination (before infection), which is more effective to confer protection against virulent pathogens such as *P. syringae* pv. *tomato* DC3000 possessing effectors to cripple MAMP signalling[6,14]. It is surprising that CLV3p–FLS2 signalling seems to have evolved to provide constitutive immune protection in the SAM but avoid the penalty from potent growth suppression associated with MAMP signalling[5,6,15,20]. A future challenge is to elucidate the precise differential downstream signalling events via the same receptor in response to different peptide ligands. Lacking the genes for antibodies and immune cell receptors in humans[29] to respond to new signals from diverse invaders, plant RLKs, displaying high polymorphism and fast evolution[30], may provide an alternative means to recognize self or non-self in a beneficial manner through constant selections in evolution. It will also be important to explore the roles of other secreted plant peptides and known or orphan receptors in innate immunity[4,6,17,30].

METHODS SUMMARY

Plasmid constructs. The constructs for expressing FLS2–haemagglutinin (HA) and BAK1–Flag for co-immunoprecipitation were reported previously[14]. LRR23b–HA and fls2-24–HA are mutant variants of the LRR domain of FLS2, which were generated by site-directed mutagenesis. The *fls2-24* allele is a Gly to Arg mutation in the 10th LRR domain of FLS2 and is insensitive to flg22 (ref. 25). LRR23b is mutated in two amino acids (Gln to Leu and Phe to Leu) in the 23rd LRR domain of FLS2 and lacks flg22 signalling[26].

Mesophyll protoplast transient assays. Protoplast isolation and transient expression assays were performed as previously described[9,14]. For protein expression in co-immunoprecipitation and in-gel kinase assays, protoplasts were transfected with plasmid DNA and incubated for 6 h at room temperature. Then, peptides such as CLV3p and flg22 were added for 10 min to induce MAPK activation or FLS2–BAK1 interaction. For qRT–PCR analysis, protoplasts were treated with peptides for 1 h.

In-gel kinase assay and co-immunoprecipitation. Both experiments were performed according to procedures previously described[9,14]. MBP (Invitrogen) was used as a substrate for endogenous MPK3 and MPK6 activation analysis[9]. For co-immunoprecipitation, FLS2–HA and BAK1–Flag were co-immunoprecipitated by an anti-Flag antibody (Sigma) and detected by an anti-HA antibody (Roche) in immunoblot analysis.

Full Methods and any associated references are available in the online version of the paper at www.nature.com/nature.

Received 9 March 2010; accepted 10 February 2011.
Published online 17 April 2011.

1. Bäurle, I. & Laux, T. Apical meristems: the plant's fountain of youth. *Bioessays* **25,** 961–970 (2003).
2. Scheres, B. Stem cells: a plant biology perspective. *Cell* **122,** 499–504 (2005).
3. Hollings, M. Disease control through virus-free stock. *Annu. Rev. Phytopathol.* **3,** 367–396 (1965).
4. Jun, J. H., Fiume, E. & Fletcher, J. C. The CLE family of plant polypeptide signaling molecules. *Cell. Mol. Life Sci.* **65,** 743–755 (2008).
5. Gomez-Gomez, L. & Boller, T. FLS2: An LRR receptor-like kinase involved in the perception of the bacterial elicitor flagellin in *Arabidopsis*. *Mol. Cell* **5,** 1003–1011 (2000).
6. Boller, T. & Felix, G. A renaissance of elicitors: Perception of microbe-associated molecular patterns and danger signals by pattern-recognition receptors. *Annu. Rev. Plant Biol.* **60,** 379–406 (2009).
7. Ishii, K. J., Koyama, S., Nakagawa, A., Coban, C. & Akira, S. Host innate immune receptors and beyond: Making sense of microbial infections. *Cell Host Microbe* **3,** 352–363 (2008).
8. Curran, S. P., Wu, X., Riedel, C. G. & Ruvkun, G. A soma-to-germline transformation in long-lived *Caenorhabditis elegans* mutants. *Nature* **459,** 1079–1084 (2009).
9. Asai, T. *et al.* MAP kinase signalling cascade in *Arabidopsis* innate immunity. *Nature* **415,** 977–983 (2002).
10. Zipfel, C. *et al.* Bacterial disease resistance in *Arabidopsis* through flagellin perception. *Nature* **428,** 764–767 (2004).
11. Yamamizo, C. *et al.* Rewiring mitogen-activated protein kinase cascade by positive feedback confers potato blight resistance. *Plant Physiol.* **140,** 681–692 (2006).
12. Yadav, R. K., Girke, T., Pasala, S., Xie, M. & Reddy, G. V. Gene expression map of the *Arabidopsis* shoot apical meristem stem cell niche. *Proc. Natl Acad. Sci. USA* **106,** 4941–4946 (2009).
13. Kondo, T. *et al.* A plant peptide encoded by *CLV3* identified by in situ MALDI-TPF MS analysis. *Science* **313,** 845–848 (2006).
14. Shan, L. *et al.* Bacterial effectors target the common signaling partner BAK1 to disrupt multiple MAMP receptor-signaling complexes and impede plant immunity. *Cell Host Microbe* **4,** 17–27 (2008).
15. Chinchilla, D. *et al.* A flagellin-induced complex of the receptor FLS2 and BAK1 initiates plant defence. *Nature* **448,** 497–500 (2007).
16. Heese, A. *et al.* The receptor-like kinase SEERK3/BAK1 is a central regulator of innate immunity in plants. *Proc. Natl Acad. Sci. USA* **104,** 12217–12222 (2007).
17. Butenko, M. A., Vie, A. K., Brembu, T., Aalen, R. B. & Bones, A. M. Plant peptides in signaling: looking for new partners. *Trends Plant Sci.* **14,** 255–263 (2009).
18. Miwa, H. *et al.* The receptor-like kinase SOL2 mediates CLE signaling in *Arabidopsis*. *Plant Cell Physiol.* **49,** 1752–1757 (2008).
19. Müller, R., Bleckmann, A. & Simon, R. The receptor kinase CORYNE of *Arabidopsis* transmits the stem cell-limiting signal CLAVATA3 independently of CLAVATA1. *Plant Cell* **20,** 934–946 (2008).
20. Zipfel, C. *et al.* Perception of the bacterial PAMP EF-Tu by the receptor EFR restricts *Agrobacterium*-mediated transformation. *Cell* **125,** 749–760 (2006).
21. Fiers, M. *et al.* The CLAVATA3/ESR motif of CLAVATA3 is functionally independent from the nonconserved flanking sequences. *Plant Physiol.* **141,** 1284–1292 (2006).
22. Felix, G., Duran, J. D., Volko, S. & Boller, T. Plants have a sensitive perception system for the most conserved domain of bacterial flagellin. *Plant J.* **18,** 265–276 (1999).
23. Bäurle, I. & Laux, T. Regulation of *WUSCHEL* transcription in the stem cell niche of the *Arabidopsis* shoot meristem. *Plant Cell* **17,** 2271–2280 (2005).
24. Chinchilla, D., Bauer, Z., Regenass, M., Boller, T. & Felix, G. The *Arabidopsis* receptor kinase FLS2 binds flg22 and determines the specificity of flagellin perception. *Plant Cell* **18,** 465–476 (2006).
25. Gómez-Gómez, L., Bauer, Z. & Boller, T. Both the extracellular leucine-rich repeat domain and the kinase activity of FLS2 are required for flagellin binding and signaling in *Arabidopsis*. *Plant Cell* **13,** 1155–1163 (2001).
26. Dunning, F. M., Sun, W., Jansen, K. L., Helft, L. & Bent, A. F. Identification and mutational analysis of *Arabidopsis* FLS2 leucine-rich repeat domain residues that contribute to flagellin perception. *Plant Cell* **19,** 3297–3313 (2007).
27. Bauer, Z., Gomez-Gomez, L., Boller, T. & Felix, G. Sensitivity of different ecotypes and mutants of *Arabidopsis thaliana* toward the bacterial elicitor flagellin correlates with the presence of receptor-binding sites. *J. Biol. Chem.* **276,** 45669–45676 (2001).
28. Guo, Y., Han, L., Hymes, M., Denver, R. & Clark, S. E. CLAVATA2 forms a distinct CLE-binding receptor complex regulating *Arabidopsis* stem cell specification. *Plant J.* **63,** 889–900 (2010).
29. Goldsby, R. A., Kindt, T. J. & Osborne, B. A. *Kuby Immunology* (W. H. Freeman, New York, 2006).
30. Clark, R. M. *et al.* Common sequence polymorphisms shaping genetic diversity in *Arabidopsis thaliana*. *Science* **317,** 338–342 (2007).

Supplementary Information is linked to the online version of the paper at www.nature.com/nature.

Acknowledgements We thank T. Laux for the *pWUS::GUS* line, Y. Matsubayashi for the purified Ara-CLV3 peptide and advice, A. Collmer for the GFP-labelled *P. syringae* pv. *tomato* DC3000, L. Shan and P. He for constructs, G. Tena, F. Ausubel, J. Bush, J. Plotnikova and ABRC for mutant seeds and bacterial strains, and Y. Xiong, M. McCormack, Y. Niu, M. Ramon and J. Li for critically reading of the manuscript. Funding was provided by the NSF, NIH and the MGH CCIB fund to J.S.

Author Contributions H.L. and J.S. initiated the project and designed the experiments; H.L. carried out the experiments and prepared the data with assistance from O.-K.C.; H.L and J.S. wrote the manuscript.

Author Information Reprints and permissions information is available at www.nature.com/reprints. The authors declare no competing financial interests. Readers are welcome to comment on the online version of this article at www.nature.com/nature. Correspondence and requests for materials should be addressed to H.L. (hrlee@molbio.mgh.harvard.edu) or J.S. (sheen@molbio.mgh.harvard.edu).

METHODS

Plasmid constructs. The constructs for expressing FLS2–haemagglutinin (HA) and BAK1–Flag for co-immunoprecipitation were reported previously[14]. LRR23b–HA and fls2-24–HA are mutant variants of the LRR domain of FLS2, which were generated by site-directed mutagenesis. The *fls2-24* allele is a Gly to Arg mutation in the 10th LRR domain of FLS2 and is insensitive to flg22 (ref. 25). LRR23b is mutated in two amino acids (Gln to Leu and Phe to Leu) in the 23rd LRR domain of FLS2 and lacks flg22 signalling[26].

Mesophyll protoplast transient assays. Protoplast isolation and transient expression assays were performed as previously described[9,14]. For protein expression in co-immunoprecipitation and in-gel kinase assays, protoplasts were transfected with plasmid DNA and incubated for 6 h at room temperature. Then, peptides such as CLV3p and flg22 were added for 10 min to induce MAPK activation or FLS2–BAK1 interaction. For qRT–PCR analysis, protoplasts were treated with peptides for 1 h.

In-gel kinase assay and co-immunoprecipitation. Both experiments were performed according to procedures previously described[9,14]. MBP (Invitrogen) was used as a substrate for endogenous MPK3 and MPK6 activation analysis[9]. For co-immunoprecipitation, FLS2–HA and BAK1–Flag were co-immunoprecipitated by an anti-Flag antibody (Sigma) and detected by an anti-HA antibody (Roche) in immunoblot analysis.

Plant materials and growth conditions. Col-0 and L*er* were used as wild-type *Arabidopsis* plants in this study. The *bak1-4*, *efr-1*, and *fls2* (*Salk_141277*) mutants are in the Col-0 background[14,15,20] and *clv1-1*, *clv2-1*, *clv3-2* and *fls2-24* are in L*er* background[5,31,32]. The *clv1-1* mutation is in the kinase domain and represents a dominant-negative allele[33]. The mutation of *clv2-1* causes the early stop codon at the 33rd residue and is a null allele[34]. The γ-ray-induced *clv3-2* is a presumed null allele[33,35]. Wild-type and mutant plants were grown on soil at 23 °C, 65% humidity, and 75 μmol m^{-2} s^{-1} light intensity under 12 h light/12 h dark photoperiod conditions for 4 weeks before mesophyll protoplast isolation[36]. For liquid culture of *Arabidopsis* seedlings, seeds were germinated and grew in 6-well plates containing 1 ml of liquid medium (0.5× MS and 0.5% sucrose, pH 5.8 adjusted with KOH). For GUS assay in the SAM and qRT–PCR analysis using SAM tissues, seedlings were grown for 8 days. For growth inhibition analysis by flg22 and CLV3p, seedlings were grown at the same condition for 8 days (Fig. 3a, b and Supplementary Fig. 8b) or 6 days (Fig. 3c–e and Supplementary Fig. 7b).

qRT–PCR analysis. Total RNA was isolated from protoplasts or SAM tissues with TRIzol reagent (Invitrogen). To harvest SAM tissues, seedlings were instantaneously frozen by liquid nitrogen in the mortar pre-chilled on the dry ice. Cotyledons, hypocotyls and roots were removed using fine forceps. The purity of the harvested SAM tissue was confirmed by SAM-specific marker genes and the absence of marker genes not expressed in the SAM (Supplementary Fig. 2)[12]. First-strand cDNA was synthesized from 1 μg of total RNA with M-MLV reverse transcriptase (Promega). All qRT–PCR analyses were performed by CFX96 real-time PCR detection system with iQ SYBR green supermix (Bio-Rad). *ACT2* (*ACTIN2*, At3g18780) was used as a control gene.

GUS staining. GUS staining was performed as described[23]. Plants were fixed in 90% cold acetone for 20 min and rinsed twice in staining buffer without X-Gluc (5-bromo-4-chloro-3-indoxyl-beta-D-glucuronide). Samples were infiltrated with staining buffer (100 mM $NaPO_4$ buffer, pH 7.0; 0.5 mM ferrocyanide; 0.5 mM ferricyanide; 0.1% Triton X-100; 10 mM EDTA, pH 8.0; 1 mM X-Gluc (Gold Biotechnology)) under vacuum for 10 min and incubated at 37 °C for 3 h. After then, staining buffer was removed and dehydrated up to 70% ethanol. Microscopic analysis was carried out with Leica DFC 500 camera mounted on Leica MZ16F.

Bacterial infection assay in the SAM. Nine seeds were sowed in 1-ml liquid medium in 6-well plates and grown under constant light (50–65 μmol m^{-2} s^{-1}) at 25–27 °C without shaking. *P. syringae* pv. *tomato* DC3000–GFP culture was grown in KB liquid medium (50 μg ml^{-1} of rifampicin and 15 μg ml^{-1} of tetracyclin) with shaking at 28 °C. Overnight cultured *P. syringae* pv. *tomato* DC3000–GFP were washed twice with water and diluted to an optical density at 600 nm (OD_{600}) of 0.02. Diluted *P. syringae* pv. *tomato* DC3000–GFP (50 μl) was added into the liquid medium with 2-day-old seedlings. Plants and bacteria were co-cultivated with gentle shaking (50 r.p.m.) for 2, 3 or 4 days under constant light. For observation of bacteria-infected SAM, co-cultivated seedlings were washed with 70% ethanol twice and rinsed twice with water. All seedlings were placed on glass slides with 1 ml of water, and squashed gently by coverslips for bacterial observation using a confocal laser-scanning microscope (Leica TCS-NT). The experiment was repeated at least five times with similar results in L*er*, *fls2-24*, *clv3-2*, *clv1-1* and *clv2-1* (Fig. 4c). For the qPCR analysis of DC3000–GFP, diluted *P. syringae* pv. *tomato* Dc3000–GFP (OD_{600} = 0.5, 200 μl) was co-cultivated with wild-type or mutant seedlings for 3 or 4 days. After washing and rinsing seedlings twice, tissues from five SAMs were harvested and ground in 100 μl of water. Control experiments were conducted at 0 days after co-cultivation to determine nonspecific bacterial attachment 1 h after co-cultivation (black bar). The experiment was repeated three times with similar results. The GFP level determined by qPCR was correlated with specific bacterial growth, and normalized based on the *Arabidopsis ACT2* gene in the SAM tissues.

Seedling pathogen assay. The protocol was modified from that previously described[37,38]. Nine seeds were sowed in 6-well plates containing 1 ml of liquid medium. Plants were grown under constant light at 25–27 °C without shaking. *P. syringae* pv. *tomato* DC3000 culture was grown in KB liquid medium (50 μg ml^{-1} of rifampicin) with shaking at 28 °C. Overnight cultured *P. syringae* pv. *tomato* DC3000 was washed twice with water and diluted to OD_{600} = 0.02, 1×10^7 c.f.u. ml^{-1}. After 6 days of seedling growth, 50 μl of diluted *P. syringae* pv. *tomato* DC3000 was added into 1 ml of fresh 0.5× MS liquid medium without sucrose. After adding *P. syringae* pv. *tomato* DC3000, plates containing plants and bacteria were co-cultivated with gentle shaking (<50 r.p.m.) for 1 day under constant light (50–65 μmol m^{-2} s^{-1}). For CLV3p- and flg22-induced immunity, seedlings were treated with 1 μM or 10 μM of CLV3p or 100 nM of flg22 peptide 1 day before adding *P. syringae* pv. *tomato* DC3000. For bacterial counting, co-cultivated seedlings were washed with 70% ethanol twice and rinsed twice with water. Then, three seedlings were put into each of three 1.5-ml tubes containing 100 μl of water and ground by a hand drill and blue pestles. After preparing serial dilutions, 10 μl of diluted bacteria (from10^{-3} to 10^{-5}) was spread on the KB plates and incubated for 2 days at 28 °C before counting.

Assay for CLV3p-mediated SAM arrest. Twenty seeds of Col-0 and *fls2* mutant were sowed in Petri dishes (100 × 25 mm) containing 10 ml of liquid medium with or without 1 μM CLV3p. Plants were grown in a growth chamber at 23 °C under short day condition (8 h light/16 h dark, 75 μmol m^{-2} s^{-1}) for 4 weeks. The SAM tissues were cut and fixed using 4% (w/v) paraformaldehyde/4% (v/v) DMSO at 4 °C overnight. Collected samples were dehydrated through ethanol series (30%, 50%, 70%, 95% for 1 h in each step) at 4 °C and stained with 0.1% Eosin Y (Sigma) in 100% ethanol at 4 °C overnight. Ethanol was changed through histoclear series (50% ethanol: 50% histoclear, 100% histoclear, 100% histoclear for 1 h in each step) (National Diagnostics). Histoclear was then gradually changed with melted paraffin (Fisher Scientific) in a 60 °C chamber. Replacement of freshly melted paraffin was performed for 4 days. Paraffin-embedded tissues were poured into the mould and adjusted in appropriated position. Section was carried out with a rotary microtome (Leica RM2255) at 8-μm thickness. Sectioned ribbons were placed on poly-prep glass slides (Sigma) with pre-warm water and incubated on a slide warmer (Fisher Scientific) at 42 °C overnight. For meristem staining, paraffin of sections was removed by 100% histoclear twice for 10 min. Sectioned tissues were hydrated through reverse ethanol series (100%, 70%, 30% ethanol and water for 2 min in each step). Sections were stained with 0.1% Giemsa (Sigma) for 5 min and rinsed briefly with water. Stained sections were dehydrated through ethanol series (2 min in each step) and transferred to 100% histoclear for 2 min. For microscopic analysis, samples were dried and mounted with Cytoseal 60 (Richard-Allan Scientific) before taking pictures using Leica DM5000B.

Direct binding assay. The protocol was modified from that previously described[27,28,39,40]. For reparation of receptor proteins, FLS2–HA, fls2-24–HA, LRR23b–HA and BRI1–HA were expressed in *fls2* protoplasts (2.5×10^5 cells) for 6 h. Protoplasts were harvested and then re-suspended in 500 μl of binding buffer (25 mM MES/KOH, pH 5.8, 3 mM $MgCl_2$, 10 mM NaCl) with 2 mM DTT and protease inhibitor (Roche). Cells were vigorously mixed by vortex and kept on ice for 5 min, and centrifuged at 10,000*g* for 20 min to yield pellet. The pellets were re-suspended in 100 μl of binding buffer and the protein concentration from re-suspended extract was measured by a NanoDrop 1000 spectrophotometer. This extract contained 50 μg of total protein. For the binding assay, re-suspended extracts (100 μl) in binding buffer were mixed with ^{125}I-Tyr-CLV3p (100 fmol in each sample) without or with unlabelled Tyr-CLV3p as a competitor for 30 min on ice. The average of specific radioactivity in five different batches of ^{125}I-Tyr-CLV3p was 2,023.52 Ci $mmol^{-1}$. ^{125}I-Tyr-CLV3p bound extracts were collected by a vacuum filtration system through glass fibre filters (Macherey-Nagel MN GF-2, 2.5-cm diameter), which were pre-incubated with 1% BSA, 1% bactotrypton, 1% bactopepton in binding buffer. Filters were washed with 15 ml of cold binding buffer and the retained radioactivity was determined by a gamma counter Beckman LS6500. Specific binding was measured by subtracting nonspecific binding (with 10–20 μM unlabelled Tyr-CLV3p competitor) from total binding (without competitor). In the saturation binding assay, the nonspecific binding in the presence of 20 μM unlabelled Tyr-CLV3p competitor showed linear increase with 1 to 100 nM ^{125}I-Tyr-CLV3p and accounted for 40–60% of total binding, which was similar to the range of nonspecific binding observed with ^{125}I-Tyr-flg22 binding to intact cells (Fig. 3a, Bauer *et al.*, 2001)[27]. The dissociation constant (K_d), Scatchard plot and the nonlinear regression analysis of competition assay were presented using the Prism 5 program (GraphPad). From the saturation data

of $B_{max} = 0.53\,pmol\,mg^{-1}$ protein and 50 µg protein from 2.5×10^5 cells, 6.36×10^4 ^{125}I-Tyr-CLV3p binding sites per cell could be estimated in total cell extracts. Specific CLV3p binding to FLS2 was similar to CLV3p binding to CLV1 and CLV2, the established CLV3p receptors[28,39].

31. Koornneef, M. *et al.* Linkage map of *Arabidopsis thaliana*. *J. Hered.* **74,** 265–272 (1983).
32. Clark, S. E., Running, M. P. & Meyerowitz, E. M. CLAVATA3 is a specific regulator of shoot and floral meristem development affecting the same processes as CLAVATA1. *Development* **121,** 2057–2067 (1995).
33. Diévart, A. *et al. CLAVATA1* dominant-negative alleles reveal functional overlap between multiple receptor kinases that regulate meristem and organ development. *Plant Cell* **15,** 1198–1211 (2003).
34. Jeong, S., Trotochaud, A. E. & Clark, S. E. The Arabidopsis *CLAVATA2* gene encodes a receptor-like protein required for the stability of the *CLAVATA1* receptor-like kinase. *Plant Cell* **11,** 1925–1933 (1999).
35. Fletcher, J. C., Brand, U., Running, M. P., Simon, R. & Meyerowitz, E. M. Signaling of cell fate decisions by *CLAVATA3* in *Arabidopsis* shoot meristems. *Science* **283,** 1911–1914 (1999).
36. Yoo, S. D., Cho, Y. H. & Sheen, J. *Arabidopsis* mesophyll protoplasts: a versatile cell system for transient gene expression analysis. *Nature Protocols* **2,** 1565–1572 (2007).
37. Schreiber, K., Ckurshumova, W., Peek, J. & Desveaux, D. A high-throughput chemical screen for resistance to *Pseudomonas syringae* in *Arabidopsis*. *Plant J.* **54,** 522–531 (2008).
38. Boudsocq, M. *et al.* Differential innate immune signaling via Ca^{2+} sensor protein kinases. *Nature* **464,** 418–422 (2010).
39. Ogawa, M., Shinohara, H., Sakagami, Y. & Matsubayashi, Y. *Arabidopsis* CLV3 peptide directly binds CLV1 ectodomain. *Science* **319,** 294 (2008).
40. Ohyama, K., Shinohara, H., Ogawa-Ohnishi, M. & Matsubayashi, Y. A glycopeptide regulating stem cell fate in *Arabidopsis thaliana*. *Nature Chem. Biol.* **5,** 578–580 (2009).